LOwer CRETAceous project, summary of results

IDA LYKKE FABRICIUS & BODIL WESENBERG LAURIDSEN

Geological Society of Denmark
https://2dgf.dk

Received 10 January 2025
Accepted in revised form 29 March 2025
Published online 7 August 2025

Fabricius, I.L. & Lauridsen, B.W. 2025. LOwer CRETAceous project, summary of results. Bulletin of the Geological Society of Denmark, Vol. 71, pp. 1–6. ISSN 2245-7070. https://doi.org/10.37570/bgsd-2025-71-01

We present summary of results from the LOCRETA project, grouped according to scientific approach: 1) Sedimentology and stratigraphy, 2) Structural geology, 3) Petrography and Petrophysics, and 4) Rock mechanics.

Keywords: Chalk, North Sea Basin, sedimentology, rock mechanics, geophysics.

Ida L. Fabricius [ilfa@dtu.dk], Department of Environmental and Resource Engineering, Technical University of Denmark, Denmark. Bodil W. Lauridsen [bwl@geus.dk]. Geological Survey of Denmark and Greenland, Denmark.

This thematic volume presents results from the LOCRETA project (2017–2021) which addressed some aspects of the Lower Cretaceous Cromer Knoll Group of the North Sea Basin. The group includes two chalk formations that host hydrocarbons in the North Sea and are subject to petroleum production: The Tuxen Formation of Hauterivian (BC 8) to Barremian (BC15) age and the Sola Formation of Barremian (BC15) to Albian (BC23–BC24) age. In the area around the Valdemar Field (central part of the Danish Central Graben, DCG), each formation is up to 100 m thick and buried to a depth of more than 2 km. The chalk is clay bearing and relatively soft, and the mechanical stability is a concern during hydrocarbon production. The interpretation of geophysical surface- and borehole data has also proven challenging, partly due to complex mineralogy and sparse information on pore water composition.

The LOCRETA project was initiated to address these rock mechanical and geophysical issues based on a revised architectural framework involving sedimentology, stratigraphy, paleontology and geochemistry. To increase our understanding of the Lower Cretaceous, a study of the nearby and equivalent Vedsted (Valanginian–Aptian/Albian) and Rødby (Aptian/Albian) formations in the Danish Basin was also included.

Sedimentology and stratigraphy

Investigations into the sedimentology and stratigraphy of the upper part of the Cromer Knoll Group, the Tuxen and Sola formations, are highly relevant for understanding the controlling factors of reservoir properties and heterogeneities (Fig. 1A). One of the aims during the LoCRETA project was to refine and better constrain the architectural framework of the Lower Cretaceous in the DCG and to understand equivalent strata of the Danish Basin. Data and interpretations presenting this part of the study have been published in the following articles: Blok *et al*. (2022, 2023), Ineson *et al*. (2022a, b), Jelby *et al*. (2022, 2024), Lauridsen *et al*. (2022) and Rudra *et al*. (2021).

The Tuxen and Sola formations comprise a heterogeneous succession of white to marly grey pelagic chalk interbedded with hemipelagic dark-grey marlstone and black marlstone (Ineson 1993, Jelby *et al*. 2022). The presence of chalk in the Hauterivian to Aptian part of the Vedsted Formation of the Danish Basin demonstrates that carbonate-rich pelagic sediments accumulated locally in the siliciclastic-dominated Danish Basin and indicates that benthic carbonate production was insignificant in this setting (Lauridsen *et al*. 2022; Fig. 1B).

A comprehensive facies analysis of the pelagic and hemipelagic carbonates has been conducted based on the cored sections of seven wells from the Lower Cretaceous Tuxen and Sola formations in the DCG (Jelby *et al*. 2022). The study identifies 50 facies based on a continuous series of six lithologies, eight sedimentary structures and two colours related to redox level (Jelby *et al*. 2022). A detailed SEM study of 22 facies identified in the Boje 2C well found that the microscopic character corresponds to the identified macroscopic sedimentary facies, and only bioturbation and shear deformation were not consistently identified (Fabricius *et al*. 2025). Diagenesis was reflected in the occurrence of calcite-cementation, silicification, pyrite, calcite-rimmed dolomite and more euhedral calcite mud particles with depth (Fabricius *et al*. 2025).

The black marlstones of early Barremian age (BC14, Munk Marl Bed), and of early Aptian age (BC18, Fischschiefer Member), are widely recognized in the North Sea subsurface and used as marker horizons (e.g. Ineson *et al*. 2022a, b); the latter is commonly correlated with the globally recognized OAE1a (Blok *et al*. 2023). In the deep Adda-1 well, the base of the Munk Marl Bed is a fractured, highly bioturbated and cemented hardground indicative of relative sea-level fall followed by laminated, organic-rich marlstone reflecting poorly oxygenated bottom waters (Ineson *et al*. 2022a). The lamination is also reflecting colour banding as shifts in the relative dominance of carbonate (nannofossils and micarb), framboidal pyrite, organic material, and clay (Ineson *et al*. 2022a). The Fischschiefer Member consists of black, finely laminated organic-rich marlstones and is typically 2 to 5 m thick (Ineson *et al*. 2022b). High-resolution clay-mineral assemblage analyses were conducted on the Lower Cretaceous marlstone and chalk of several cores from the Danish Central Graben to evaluate potential source areas of the detrital material, to understand the palaeogeographic evolution and to obtain more information on the climatic evolution during Early Cretaceous in the Boreal Realm (Blok *et al*. 2022, 2023).

In clay-rich marl samples, kaolinite is the dominant clay mineral and calcite particles are separated and embedded in clay (Blok *et al*. 2023). In more calcite-rich samples, the particles are in full contact (Fabricius *et al*. 2025).

The formations represent an overall gradual change from siliciclastic- to carbonate-dominated sedimentation attributed to a regional sea-level rise culminating in the Late Cretaceous eustatic highstand (Michelsen *et al*. 1987; van Buchem *et al*. 2018). An updated depositional model was published identifying four major depositional sequences, recording 20 Myr of transgressive-regressive cycles from 1) late Hauterivian to earliest Barremian highstand (Fig. 1B), 2) early Barremian inversion and lowstand controlled basin-isolation with reduced water circulation (Munk Marl Bed) (Fig. 1C), followed by late Barremian highstand and deposition of clean chalk, 3) latest Barremian lowstand and finally early Aptian transgression (transgression-controlled anoxia during Fischschiefer Member), 4) late Aptian highstand and latest Aptian to earliest Albian lowstand (Jelby *et al*. 2024). The depositional model correlates to the four depositional units identified in the Hauterivian to Aptian Vedsted and Rødby formations in the Danish Basin (Lauridsen *et al*. 2022).

The distribution of kaolinite in the different wells

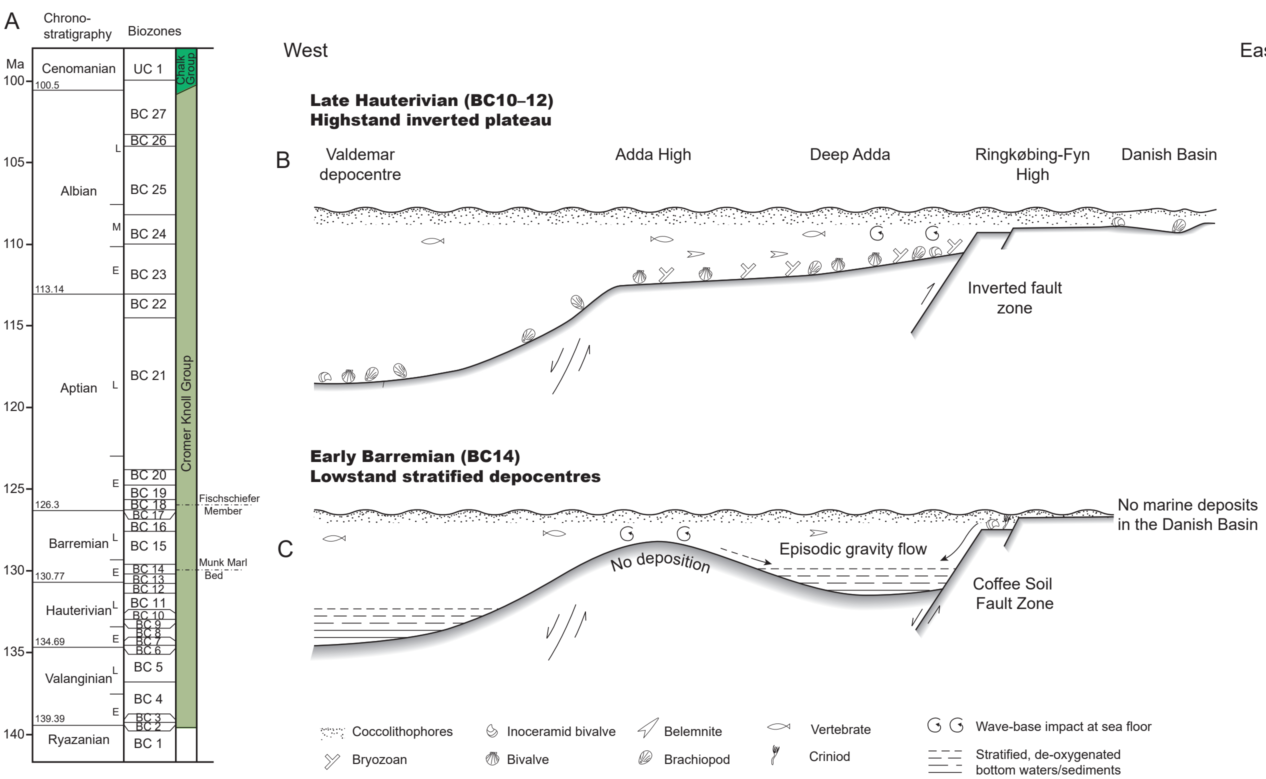

Fig. 1. A. Stratigraphic chart of the Lower Cretaceous Cromer Knoll Group from Jelby *et al*. (2022). The biozones are based on nannofossils. **B-C.** Schematic palaeo-environmental reconstructions of the DCG and Danish Basin contrasting the Late Hauterivian highstand with the earliest Barremian lowstand (modified from Ineson *et al*. 2022a and Lauridsen *et al*. 2022). Note that the different wells studied in the LoCRETA project occur within the Valdemar depocentre (e.g. North Jens-1), the Adda High (Adda-cores), the Deep Adda area (Deep Adda-1) and the Danish Basin (e.g. Vinding-1 and Haldager-1).

suggests a clay source located in the southwestern part of the DCG (Blok *et al*. 2023). The overall decrease in kaolinite in the DCG from the late Hauterivian to the late Barremian indicates a climatic change towards drier conditions with some minor, slightly more humid periods (Blok *et al*. 2023).

Structural geology

Using seismic data for unravelling the pattern of faults and fractures in the Valdemar Field area is relevant, not least for the detection of open fractures that are possible fluid conduits, or conversely sealed clay-bearing fractures that can potentially enclose pressure departments in the petroleum bearing intervals. Results from the PRIORITY research programme (1997–2002) found this task too complex (Madsen & Britze 1999, as cited in Lorentzen *et al*. 2022a), in part due to the limited seismic resolution aggravated by interfering signals from the overlying Upper Cretaceous chalk (Bredesen *et al*. 2021). In order to enhance the information gained from seismic sections and horizons, Lorentzen *et al.* (2022a) used a convolution neural network (CNN) method to map out possible fractures, and concluded that the method could help but not replace manual interpretation.

Another approach to assist seismic interpretation is to calibrate rock physical methods to borehole data. Lorentzen *et al*. (2022b) focused on modelling shear velocity, V_s from P-wave, V_P velocity data. This is relevant because if bulk density, V_P and V_S are known, the elastic moduli can be calculated, and elasticity and composition of pore fluids can be modelled. Lorentzen *et al*. (2022b) used a supervised learning approach and found the results to be possibly more precise than the results from the more conventional rock physical isoframe model. Rock physical interpretation is facilitated when the elastic moduli of the constituting minerals are known. This is of little concern in rocks with simple mineralogy, but for the clay-bearing chalks of Tuxen and Sola formations, the concern is high, and consequently Meireles & Fabricius (2023) developed an isoframe based method for modelling mineral moduli logs from well data, where both V_P and V_S have been measured.

The presence of fractures can be directly observed in borehole image logs or borehole cores. Glad *et al*. (2022) performed a detailed fracture study on cores from the Valdemar Field. They found that the most prevalent fractures are open fractures with plumose structure and hackle marks followed by small-offset shear fractures, shear fractures and rubble zones. Cemented fractures and deformation bands were found to be less dominant. Flow-enhancing fractures were found with the following densities: 7.2/m in chalk, 5.0/m in slightly marly chalk, 3.1/m in marly chalk and 4.8/m in chalky marlstone. No fractures were observed in the marlstones. A substantial number of the fractures seen to be open in cores seem not to be coated with cementing crystals and could thus possibly be closed or absent under reservoir conditions.

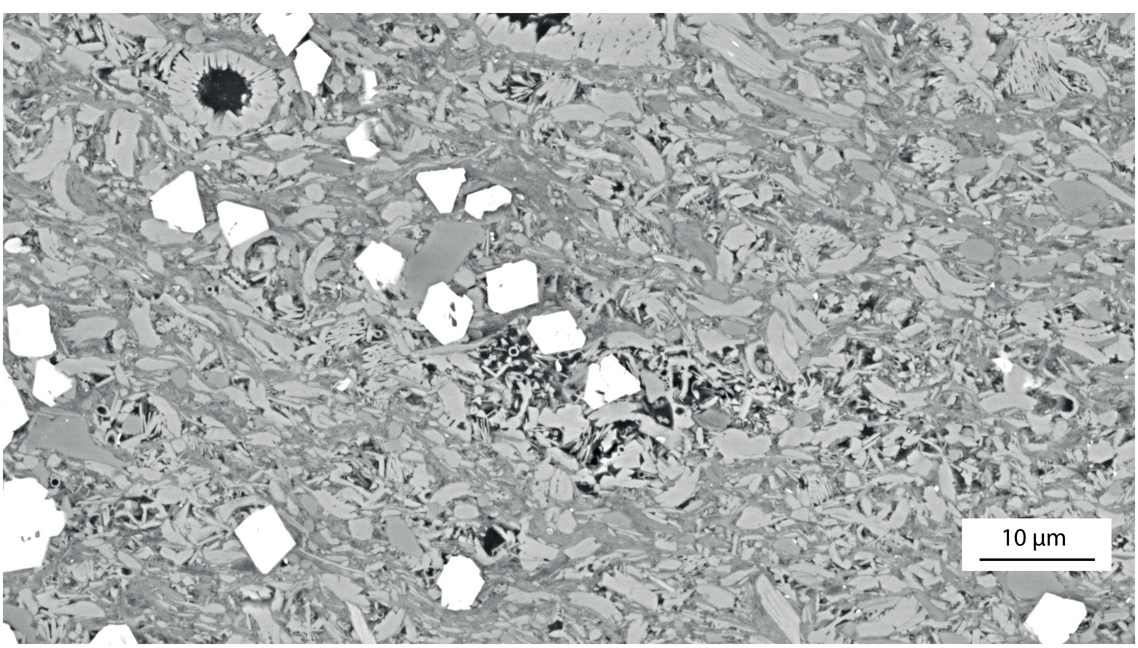

Fig. 2. Backscatter electron micrograph of polished vertical sample from well Boje-2C, 8388′4″, Lower Sola Formation. The sample has carbonate content of 79%, porosity of 27% and Klinkenberg permeability of 0.02 mD (Storebø *et al.* 2022a). White crystals are diagenetic pyrite; light grey particles are mainly (?) biogenic calcite, some are recognizable nannoconids. Medium grey distinct particles are quartz silt; darker grey silt-size and clay size particles are mainly detrital kaolinite. Black is porosity, mainly interparticlar, but also intrafossil in nannoconids. The clay is heterogeneously distributed among calcitic particles (Photo: Morten Leth Hjuler).

Petrography and petrophysics

Blok *et al.* (2023) undertook a comprehensive mineralogical study of the Tuxen and Sola formations in the North Jens-1 core. They found a dominating but varying content of calcite and that the non-carbonates primarily constitute covarying quartz and kaolinite. They also identified minor contingents of other clay minerals as well as sporadic occurrence of pyrite and dolomite. Petrographic description of backscatter electron micrographs indicate that the calcite probably primarily forms biogenic micritic particles, some recognisable nannoconids, and rare planktonic microfossils. The quartz and kaolinite represent detrital silt and clay. Porosity is almost exclusively interparticular, although nannoconids contain intrafossil porosity (Fabricius *et al.* 2025; Fig. 2). Probably due to over-pressure, the porosity is high (20–45%) (e.g. Jakobsen *et al.* 2004). These authors noticed that when cross-plotting porosity and insoluble residue, data representing the Sola Formation fall on a 10 p.u. higher trend than data representing the Tuxen Formation. Fabricius *et al.* (2025) noticed a depth-trend in diagenetic recrystallization of calcite, causing the deeper samples into closer packing. This smoothing of particles could cause samples from Tuxen Formation to have lower porosity for a given insoluble residue and higher permeability for a given porosity.

Estimating the content of hydrocarbons from porosity, ϕ, and water saturation, S_w, is a key part of petrophysics. When porosity has been assessed from radioactive logs, water saturation can be derived from electrical resistivity, R_t, by using Archie's equation directly or in modified versions. Archie's equation states $S_w^{\ n} = (R_w/(R_t\ \phi^m))$, where R_w is electrical resistivity of the pore water. The parameters m and n can be measured by core analysis. Consistent interpretation of logging data for the Tuxen and Sola

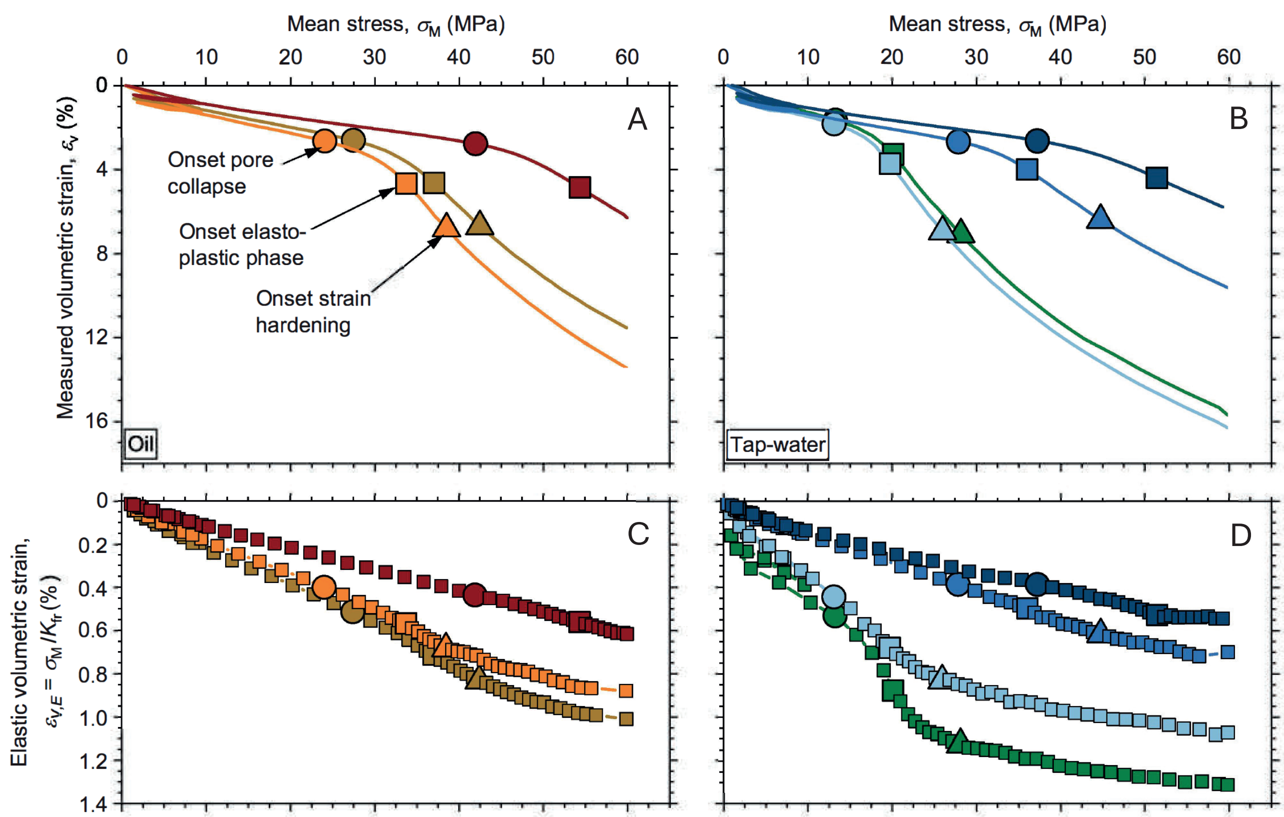

Fig. 3. Results from rock mechanical testing under hydrostatic stress conditions. Pore fluid was drained out of samples during testing. The samples were cut from three horizontal drill cores: 1) dark blue symbols, non-carbonate content 37% and porosity 31%, 2) red and medium blue symbols, non-carbonate content 21% and porosity 37%, 3) olive, orange, green and light blue symbols, non-carbonate content 12% and porosity 44%. **A**. During increasing hydrostatic/mean stress (σ_M) the oil saturated samples deform close to linearly by a volumetric strain, ε_v, until the frame of the rock starts breaking down (Onset pore collapse) at a mechanical strain of 2.5%. When the frame of the samples has practically disintegrated into particles at a strain of *c*. 5% (Onset elastoplastic phase) the increasing stress causes particles into a denser packing. At a mechanical strain of 7% (Onset strain hardening) stress must increase at an increasing rate to cause denser packing. **B**. For water saturated samples we find similar transitions among deformation phases as for the oil saturated samples and at similar strain, but the transitions take place at significantly lower stress for the water saturated samples than the oil saturated samples. **C**, **D**. Strain calculated from elastic wave velocities and mean stress, $\varepsilon_{v,E}$ is markedly lower than mechanically measured strain. (Modified after Orlander & Christensen 2024).

formations has proven difficult; Fabricius *et al*. (2005) accepted water saturations above 100%, whereas Storebø *et al*. (2022b) obtained consistent results by assuming a possibly unrealistically low R_w, and a significant contribution from pyrite to the electrical conductivity. A new approach based on specific surface measured on cuttings or cores was advocated by Proestakis *et al*. (2025) and Proestakis & Fabricius (2025). At the probably relatively high pore water salinity in the studied formations, the specific surface is covered by an adsorbed layer in which the concentration of hydrated ions is so high that it does not conduct the electrical current. When the volume of this adsorbed water is subtracted from the porosity, the water saturation can be calculated by using the theoretical value of m = 1.5.

Rock mechanics

Rock mechanical testing on chalk samples from the Tuxen Formation of the Valdemar Field was done in order to assess possible compaction development during hydrocarbon production. Laboratory tests included hydrostatic stress loading (Orlander & Christensen 2024) as well as loading involving uniaxial strain where axial stress is increased, but lateral strain is prevented by lateral stress-increase (Orlander & Christensen 2025). The tests were done on water saturated samples and on samples saturated with laboratory oil. Testing results led to the new insight that mechanical pore collapse happens at a specific and critical elastic strain of the rock irrespective of porosity or pore fluid (Fig. 3). This finding makes mineralogical sense because calcite supports the rock frame in all samples, so that it is the calcite crystal contacts that break at a critical strain of the calcite crystals.

Strain measured mechanically during testing includes both elastic strain and plastic strain, and before the onset of pore collapse, the plastic strain arises due to closure of microcracks. They are unloading cracks present in rocks that have been exhumed (*e.g*. Glad *et al*. 2024). After pore collapse, plastic strain reflects the particles becoming more densely packed. The stress causing the deformation is transmitted via the elastic strain of the particles, so in order to calculate the elastic strain, elastic wave velocities were measured throughout the testing. When mineralogy and pore fluid composition are known, we can calculate the bulk modulus of the rock frame, K_{fr}, and then elastic strain (Figs 3C, 3D; Orlander & Christensen 2024). Under hydrostatic conditions, pore collapse happens at an elastic strain of 0.4% (Figs 3C, 3D), and under uniaxial strain conditions, pore collapse happens at an elastic strain of 0.2–0.25% (Orlander & Christensen 2025). This focus on elastic strain is relevant for assessing the risk of pore collapse from logging data. A simple methodology for this assessment is given in Fabricius & Meireles (2025).

Although the onset of pore collapse is controlled by a given elastic strain irrespective of pore fluid, the collapse happens at significantly lower stress when the chalk is water saturated, than when it is oil saturated (Fig. 3). This so called "water weakening" has been noticed by numerous workers, but the present study shows that in terms of strain, the chalk is not weaker when water saturated.

Acknowledgements

We gratefully acknowledge the Danish Underground Consortium (TotalEnergies E&P Denmark, Noreco and Nordsøfonden) for granting permission to publish this work. The study was funded by the Danish Offshore Technology Centre (DTU Offshore). Tobias Orlander, Geo, is thanked for rock mechanical information (Fig. 3). Tobias Orlander, Ermis Proestakis and Michael Welch are thanked for constructive comments on parts of the manuscript.

References

Blok, C., Ineson, J., Anderskouv, K., Fantasia, A., Sheldon, E., Thibault, N., Jelby, M.E., Adatte, T. & Bodin, S. 2022: Latitude-dependant climate changes across the Aptian Oceanic Anoxic Event 1a. Palaeogeography, Palaeoclimatology, Palaeoecology 601, 111085. https://doi.org/10.1016/j.palaeo.2022.111085

Blok, C.N., Adatte, T., Ineson, J.R., Sheldon, E., Jelby, M.E., Smit, F.W.H., Lauridsen, B.W., Anderskouv, K. & Bodin, S. 2023.: Clay mineral assemblages as a tool in source-to-sink studies: an example from the Lower Cretaceous of the North Sea Basin. Bulletin of the Geological Society of Denmark 71, 99–113. https://doi.org/10.37570/bgsd-2023-71-06

Bredesen, K., Lorentzen, M., Nielsen, L. & Mosegaard. K. 2021: Quantitative seismic interpretation of the Lower Cretaceous reservoirs in the Valdemar Field, Danish North Sea. Petroleum Geoscience 27, 2021-016, 17 pp. https://doi.org/10.1144

Fabricius, I.L. & Meireles, L.P.T. 2025: Assessment of pore collapse in North Sea Lower Cretaceous carbonates using downhole elastic strain. Bulletin of the Geological Society of Denmark 71, 115–125. https://doi.org/10.37570/bgsd-2025-71-07.

Fabricius, I.L., Olsen, C. & Prasad, M. 2005: Log interpretation of marly chalk, the Lower Cretaceous Valdemar Field, Danish North Sea: application of iso-frame and pseudo water film concepts. The Leading Edge 24, 496–505.

Fabricius, I.L, Hjuler, M.L., Jelby, M.E. & Anderskouv, M. 2025: Microscopic character of the Lower Cretaceous Tuxen and Sola Formations in the Boje-2C well, central North Sea. Bulletin of the Geological Society of Denmark 71, 127-159. https://doi.org/10.37570/bgsd-2025-71-08

Glad, A.C., Amour, F., Welch, M.J., Clausen, O.R., Anderskouv, K., Ineson, J.R., Sheldon, E. & Nick, H.M. 2022: Natural fractures and discontinuities in a Lower Cretaceous chalk-marlstone reservoir, Valdemar Field, Danish North Sea. Marine and Petroleum Geology 136 105445. https://doi.org/10.1016/j.marpetgeo.2021.105445

Glad, A.C., Afrough, A., Amour, F., Ferreira, C.A.S., Price, N., Clausen, O.R. & Nick, H.M. 2023: Anatomy of fractures: Quantifying fracture geometry utilizing X-ray computed tomography in a chalk-marl reservoir; the Lower Cretaceous Valdemar Field (Danish Central Graben). Journal of Structural Geology 174, 104936. https://doi.org/10.1016/j.jsg.2023.104936

Glad, A.C., Orlander, T., Fabricius, I.L., Clausen, O.R. & Clemmensen, L.B. 2024: Characteristics and formation of natural fractures in a silica-rich chalk, Coniacian Arnager Limestone Formation, Bornholm, Denmark. Bulletin of the Geological Society of Denmark 73, 157–173. https://doi.10.37570/bgsd-2024-73-09

Ineson, J.R. 1993: The Lower Cretaceous chalk play in the Danish Central Trough. In: Parker, J.R. (Ed.), Petroleum Geology of Northwest Europe: Proceedings of the 4th Conference. Petroleum Geology Conference Series. Vol. 4. Geological Society, London, pp. 175–183. https://doi.org/10.1144/0040175.

Ineson, J.R., Lauridsen, B.W. Lode, S., Sheldon, E., Sørensen, H.O., Wisshak, M. & Anderskouv, M. 2022a: A condensed chalk-marl succession on an Early Cretaceous intrabasinal structural high, Danish Central Graben: implications for the sequence stratigraphic interpretation of the Munk Marl Bed. Sedimentary Geology 440, 106–234. https://doi.org/10.1016/j.sedgeo.2022.106234

Ineson, J.R., Petersen H.I., Andersen, C., Bjerager, M., Jakobsen, G.C., Kristensen, L., Mørk, F. & Sheldon, E. 2022b: Early Cretaceous stratigraphic and basinal evolution of the Danish Central Graben: a review. Bulletin of the Geological Society of Denmark 71, 75–98. https://doi.org/10.37570/bgsd-2022-71-05

Jakobsen, F., Ineson, J.R., Kristensen, L. & Stemmerik, L. 2004: Characterization and zonation of a marly chalk reservoir: the Lower Cretaceous Valdemar Field of the Danish Central Graben. Petroleum Geoscience 10, 21–33.

Jelby, M.E., Ineson, J.R., Thibault, N., Bodin, S., Blok, C.N., Edvardsen, N., Clemmensen, T.S., Buls, T. & Anderskouv, K. 2022: Facies and depositional processes of Lower Cretaceous carbonates, Danish Central Graben. Bulletin of the Geological Society of Denmark 71, 51–74. ISSN 2245-7070. https://doi.org/10.37570/bgsd-2022-71-04

Jelby, M.E., Ineson, J.R., Sheldon, E. & Anderskouv, M. 2024: Old chalk, new tricks: revisiting the Lower Cretaceous carbonates of the Danish Central Graben. In Hart et al. (Eds). Cretaceous Project 200 Volume 2: Regional Studies. Geological Society, London, Special Publications, 545, 1–25. https://doi.org/10.1144/SP545-2023-134

Lauridsen, B.W., Lode, S., Sheldon, E., Frykman, P., Anderskouv, K. & Ineson, J. 2022: Lower Cretaceous (Hauterivian–Aptian) pelagic carbonates in the Danish Basin: new data from the Vinding-1 well, central Jylland, Denmark. Bulletin of the Geological Society of Denmark 71, 7–29. https://doi.org/10.37570/bgsd-2022-71-02

Lorentzen, M.C.L., Bredesen, K., Smit, F.W.H., Hansen, T.H., Nielsen, L. & Mosegaard, K. 2022a: Mapping Cretaceous faults using a convolutional neural network – A field example from the Danish North Sea. Bulletin of the Geological Society of Denmark, 71, 31–50. ISSN 2245-7070. https://doi.org/10.37570/bgsd-2022-71-03

Lorentzen, M., Bredesen, K., Mosegaard, K. & Nielsen, L. 2022b: Estimation of shear sonic logs in the heterogeneous and fractured Lower Cretaceous of the Danish North Sea using supervised learning. Geophysical Prospecting 70, 1410–1431. https://doi.org/10.1111/1365-2478.13252

Madsen, L. & Britze, P. 1999: PRIORITY - Improved oil recovery and productivity from Lower Cretaceous Carbonates – EFP- 97. Sub-project 1.4.a: Seismic interpretation of the Cretaceous in the Valdemar Area. The Geological Survey of Denmark and Greenland.

Meireles, L.T.P. &. Fabricius, I.L. 2023: Deriving mineral moduli of the noncarbonate fraction in a marly chalk reservoir using petrophysical logging data and an isoframe model. Geophysics 88, D411-D425. https://doi.org/10.1007/s00603-025-04691-6

Michelsen, O., Frandsen, N., Holm, L., Jensen, T.F., Møller, J.J. & Vejbæk, O.V. 1987: Jurassic - Lower Cretaceous of the Danish Central Trough; – depositional environments, tectonism, and reservoirs. Danmarks Geologiske Undersøgelse, Serie A, 16, 44 pp. https://doi.org/10.34194/seriea.v16.7035

Orlander, T. & Christensen, H.F. 2024: Compaction phases and pore collapse in Lower Cretaceous chalk – insight from Biot's coefficient. Rock Mechanics and Rock Engineering. https://doi.org/10.1007/s00603-024-03963-x

Orlander, T. & Christensen, H.F. 2025: Elastic and plastic deformation of Lower Cretaceous North Sea Chalk during stress and time-dependent uniaxial strain compaction. Rock Mechanics and Rock Engineering. https://doi.org/10.1007/s00603-025-04691-6

Proestakis, E., Meireles, L.T.P. & Fabricius, I.L. 2025: Complex conductivity of diatomites and chalks. Geophysics 90, M181-M202. https://doi.org/10.1190/geo2024-0372.1

Proestakis, E. & Fabricius, I.L. 2025: Log interpretation for petrophysical and elastic properties of fine-grained sedimentary rocks. Petrophysics.

Rudra, A., Sanei, H., Nytoft, H.P., Petersen, H.I., Blok, C., Bodin, S. & Bojesen-Koefoed, J.A. 2021: Organic matter characterization of the Lower Cretaceous tight reservoirs in the Danish North Sea. International Journal of Coal Geology 238, 103714. https://doi.org/10.1016/j.coal.2021.103714

Storebø, E., Hjuler, M.L. & Fabricius, I.L. 2022a: Permeability modeling in clay rich carbonate reservoir. Petrophysics 63, 141 – 170. https://doi.org/10.30632/PJV63N2-2022a2

Storebø, E.M., Hjuler, M.L., Meireles, L.T.P. & Fabricius, I.L. 2022b: Effect of pyrite in water saturation evaluation of clay-rich carbonate. Petrophysics 63, 172–198. https://doi.10.30632/PJV63N2-2022a3

van Buchem, F.S.P., Smit, F.W.H., Buijs, G.J.A., Trudgill, B. & Larsen, P.H. 2018: Tectonostratigraphic framework and depositional history of the Cretaceous-Danian succession of the Danish Central Graben (North Sea) – new light on a mature area. In: Bowman, M., Levell, B. (Eds.), Petroleum Geology of NW Europe: 50 Years of Learning – Proceedings of the 8th Petroleum Geology Conference. https://doi.10.1144/PGC8.24